Ultrafast Dynamics of the Isolated Adenosine-5′-triphosphate Dianion Probed By Time-Resolved Photoelectron Imaging

Maria Elena Castellani[1], Davide Avagliano[2], and Jan R. R. Verlet[*1]

[1]*Department of Chemistry, Durham University, DH1 3LE Durham, United Kingdom.*

[2]*Institute of Theoretical Chemistry, Faculty of Chemistry, University of Vienna, Währinger Str. 17 1090 Vienna, Austria.*

Abstract

The excited state dynamics of the doubly deprotonated dianion of adenosine-5'-triphosphate, $[ATP–H_2]^{2–}$, has been spectroscopically explored by time-resolved photoelectron spectroscopy following excitation at 4.66 eV. Time-resolved photoelectron spectra show that two competing processes occur for the initially populated $^1\pi\pi^*$ state. The first is rapid electron emission by tunneling through a repulsive Coulomb barrier as the $^1\pi\pi^*$ state is a resonance. The second is nuclear motion on the $^1\pi\pi^*$ state surface leading to an intermediate that no longer tunnels and subsequently decays by internal conversion to the ground electronic state. The spectral signatures of the features are similar to those observed for other adenine-derivatives, suggesting that this nucleobase is quite insensitive to the nearby negative charges localized on the phosphates, except of course for the appearance of the additional electron tunneling channel which is open in the dianion.

Correspondence:

[*]j.r.r.verlet@durham.ac.uk

Introduction

DNA, together with its building-blocks and derivatives, represents one of the most important molecules of biological interest.[1] DNA has a high stability imparted by hydrogen bonding and π-stacking such that it is chemically unreactive. However, DNA can undergo significant damage when exposed to radiation or oxidizing agents.[2, 3] Specifically, photo-oxidative damage represents one of the major causes of stress for the nucleobases, which can easily absorb ultraviolet light via their optically bright $^1\pi\pi^*$ states.[3] Despite this, the photo-induced damage quantum yield of DNA is less than 1%. This intrinsic photostability of the nucleobases arises from their non-radiative decay mechanisms.[4, 5] Consequently, there has been extensive experimental as well as theoretical work aimed at understanding the relaxation pathways of nucleobases following UV excitation. Adenine in particular has been the focus of much research, especially through gas-phase spectroscopy,[6, 7] where it has been studied as an isolated nucleobase,[8-11] but also as part of more complex structures, such as nucleotides and oligonucleotides.[12-15]

Adenosine-5'-triphosphate (ATP) is one of the most important adenine derivatives because of its pivotal role in intramolecular energy transfer. Due to the presence of three phosphate groups, ATP is generally negatively charged which can in principle affect its photo-physics. In the gas-phase, for example, the doubly-deprotonated form of ATP, $[ATP–H_2]^{2–}$, is most readily generated by electrospray ionization. Isolated dianions like $[ATP–H_2]^{2–}$ (and polyanions more generally) have a Repulsive Coulomb Barrier (RCB), [16-19] that comes about from a balance between the long-range repulsive interaction between an electron and the mono-anion and the short-range attraction that forms the dianion. The RCB can be conveniently studied using photoelectron spectroscopy as the outgoing electron is naturally sensitive to the RCB and represents a barrier that needs to be overcome in order to successfully detach an electron from the molecule. From an electronic structure perspective, excited states of the dianion can lie above the adiabatic detachment energy (ADE) but below the RCB threshold. This therefore renders the excited state a resonance that is metastable towards electron tunneling through the RCB. The RCB has been the focus of multiple theoretical[17,

[18, 20] and experimental studies;[19, 21] In particular, photoelectron spectroscopy and, more specifically, photoelectron imaging, have emerged as useful tools to probe the photo-physics of multiply charged anionic species.[16, 19, 22-27]

Anionic DNA fragments and derivatives have been the subject of multiple spectroscopy studies in the past.[12-15, 25, 28-38] Specifically, $[ATP–H_2]^{2–}$ has been probed by the Kappes group[31] and the Dessent group,[34] using photoelectron and photo-detachment action spectroscopy, respectively. We recently added to this work[13] using photoelectron imaging. Following excitation of $[ATP–H_2]^{2–}$ with 4.66 eV light, we observed electron emission from the $^1\pi\pi^*$ states on the nucleobase. The emission was directional and, in combination with theory, we could correlate this directionality to the nature shape of the RCB which peaks strongly around the negatively charged phosphates. We also provided evidence that the emission arose from electron tunneling through the RCB. That is to say that the $^1\pi\pi^*$ state excited at 4.66 eV in $[ATP–H_2]^{2–}$ is a resonance. Part of this evidence was produced using time-resolved photoelectron yield measurements. Here, we add to our previous study and we report on the time-resolved photoelectron spectra. This allows us to spectroscopically distinguish between electron tunneling and nuclear dynamics on the excited $^1\pi\pi^*$ state, which ultimately leads to internal conversion back to the ground electronic state of $[ATP–H_2]^{2–}$. It also serves as a comparison between the $^1\pi\pi^*$ state dynamics in $[ATP–H_2]^{2–}$ and in deoxy-adenosine monophosphate ($dAMP^–$)[12, 39] and bare adenine (Ade)[8-10, 38, 40-49].

Methods

The details of the anion photoelectron imaging instrument are reported elsewhere.[50, 51] $[ATP–H_2]^{2–}$ anions were generated by electrospray ionization (ESI) of a ~1 mM methanolic solution of adenosine-5′-triphosphate disodium salt (Sigma Aldrich, UK) and introduced in the first vacuum region of the instrument. The negative ions were subsequently guided by a potential gradient through a series of ring-electrode ion guides, which culminated in a pulsed ion trap. Ions were ejected and focused into a colinear Wiley–McLaren time-of-flight mass spectrometer[52] operating at 100 Hz. At the focus of the mass-spectrometer, a mass-selected ion packet was intersected with laser pulses obtained from a commercial Ti:Sapphire laser (Spectra Physics). The fundamental at 1.55 eV was used as a probe pulse. Its third harmonic at 4.66 eV served as the pump pulse and was generated by frequency doubling in a BBO (type I) crystal followed by a calcite plate, a half-waveplate and a second BBO (type I) crystal to mix the fundamental and second harmonic. Pump and probe pulses we delayed with respect to each other using a motorized delay stage. The time-resolution in the interaction region was ~100 fs. Upon irradiation of the ion packet, the ejected photoelectrons were collected and imaged by a perpendicular velocity-map imaging (VMI) arrangement.[53] Photoelectron spectra were extracted from the raw images using onion peeling in polar coordinates.[54] The photoelectron spectrum of $I^–$ was used to calibrate the VMI spectrometer. The spectral resolution was approximately ~5% of the electron kinetic energy, eKE.

The pump light at 4.66 eV is sufficiently high in energy to cause significant PE noise from photon striking the VMI electrodes. To minimize this, we coated the electrodes with platinum, which has a work function of ~4.6 eV.[55] The reduction of noise is approximately an order of magnitude at $h\nu$ = 4.66 eV. Additionally, PE images were collected both in the presence and absence of ions (by closing the ion trap) at ~1 Hz and actively subtracted. This removes the background photoelectron noise contribution from the image and also leads to larger ion signal levels. The latter arises because the loading rate of the trap is too low to fill the trap completely before it is emptied at 100 Hz. Hence,

when allowed to accumulate in the ions off cycle, there are many more ions to be extracted from the trap.

Results and analysis

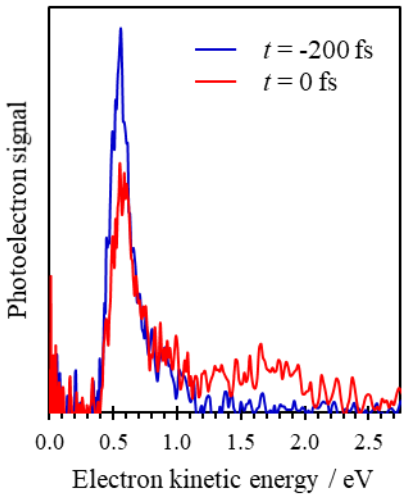

Figure 1: Time-resolved photoelectron spectra of $[ATP–H_2]^{2-}$ taken at $t = -200$ fs (blue) and 0 fs (red).

Figure 1 shows two pump-probe photoelectron spectra at delays of t = –200 fs and 0 fs. Because the probe photon energy ($h\nu_{pr}$ = 1.55 eV) is well below any excited states and the detachment threshold for $[ATP–H_2]^{2-}$, the $t = -200$ fs PE spectrum is identical to the single-photon spectrum that we have acquired at $h\nu_{pu}$ = 4.66 eV. The intense feature centered at eKE = 0.55 eV has been assigned to tunneling emission through the RCB following excitation to the $^1\pi\pi^*$ states.[13] When the pump and probe pulses overlap in time (t = 0 fs), the feature at eKE = 0.55 eV is depleted and a new feature is seen at higher eKE that extends to eKE ~ 2 eV.

Figure 2 shows a selection of the time-resolved photoelectron spectra of $[ATP–H_2]^{2-}$ in the $-200 \leq t \leq +300$ fs range, where each spectrum has had an average of the spectra with $t \leq -200$ fs subtracted to show only the time-resolved spectral changes. Additionally, to remove high-frequency

noise in the spectra, a moving average (10-point) has been applied to the photoelectron spectra. Figure 2 shows three distinct features that evolve as a function of pump-probe delay; these have been highlighted in Figure 2 as shaded regions. The peak at eKE = 0.55 eV shows a negative signal that arises from the depletion seen in the photoelectron spectra shown in Figure 1. This depletion signal recovers rapidly and has essentially recovered fully by ~300 fs. At higher energy, there is a positive signal that decays as a function of pump-probe delay, but also appears to shift towards lower eKE. Shifts in eKE can arise from changing Franck-Condon factors associated with vibrational wavepacket dynamics along an excited state potential energy surface and/or from changes in electronic state following a nonadiabatic transition.

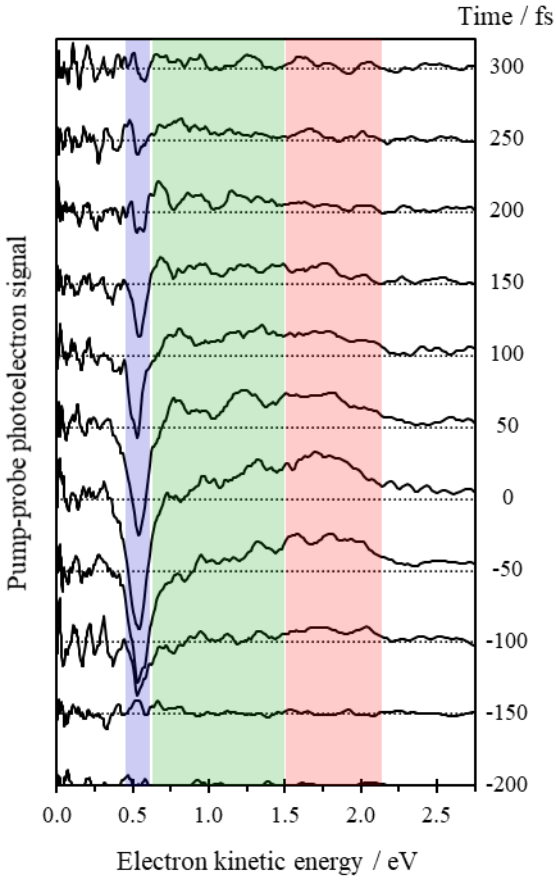

Figure 2: Time-resolved photoelectron spectra of $[ATP–H_2]^{2-}$ taken from −200 fs to +300 fs and plotted in terms of eKE. An average of the spectra at $t \leq -200$ fs was used for background subtraction.

The dynamics were analyzed using two approaches. First, the integrated photoelectron signal over three spectral windows in Figure 2 were taken and are shown in Figure 3. Also shown is the total integrated signal. The spectral windows 0.45 < eKE < 0.60 eV, 0.60 < eKE < 1.50 eV, and 1.50 < eKE < 2.10 eV are representative of the dynamics associated with the depletion, the high eKE feature and the red-shifted positive feature, respectively. These data clearly show that the high eKE feature is associated with depletion of the peak at 0.55 eV and that there is a second feature that appears and decays in the 0.6 < eKE < 1.5 eV spectral range. We can approximate that the fastest component at high eKE (which is concerted with the depletion recovery) occurs on a timescale similar to, or lower than, the cross-correlation between pump and probe pulses, *i.e.* <100 fs. The intermediate signal decays to a value of 1/*e* at ~300 fs. The key limitation with the analysis shown in Figure 3 is that there is significant spectral overlap between the differing features such that it is difficult to assess the overall spectral shape of the individual contributions.

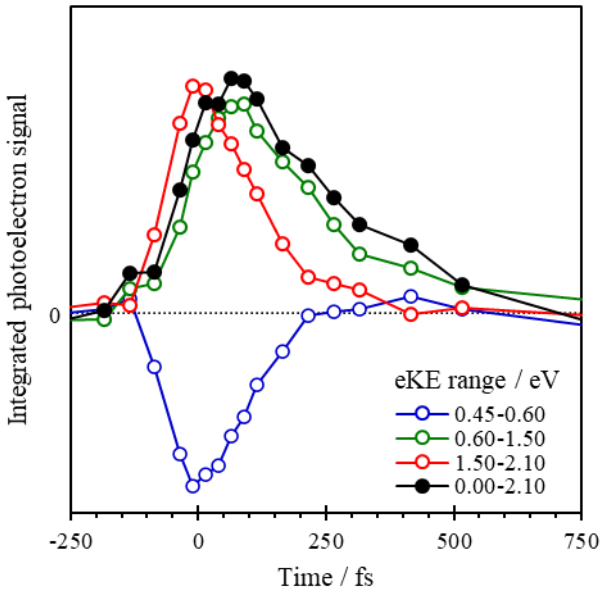

Figure 3: integrated photoelectron signal plotted as function of time over four different energy ranges.

As a second analysis method, a global fit to the time-resolved data was performed. The global fit has the form $f(\mathrm{eKE},t)=\sum_i g(t)\otimes c_i(\mathrm{eKE})\exp(-t/\tau_i)$, where c_i(eKE) represent photoelectron spectra that are associated with specific decays with lifetime τ_i (so-called decay-associated spectra). These are convoluted with the instrument response function, $g(t)$ (the cross-correlation of pump and probe pulses, which is assumed to be a Gaussian function with full-width at half-maximum of 100 fs). The minimum number of decays required to fit the data was two. In other words, the data are best represented by a 3-state model $1 \rightarrow 2 \rightarrow 3$, in which 1 and 2 are observable and 3 is some final state that cannot be probed by the current experiment.

Figure 4 shows that the photoelectron spectra associated with decays τ_1 and τ_2, where τ_1 = 54 ± 50 fs and τ_2 = 211 ± 100 fs. The first is within the time-resolution of the experiments and so should be taken as τ_1 < 100 fs. The kinetics are consistent with those estimated from Figure 3. The τ_1-associated spectrum has positive signal at 1.2 < eKE < 2.3 eV and negative signal between 0.4 < eKE < 1.2 eV. Positive signal corresponds to signal decaying with a lifetime of τ_1, while negative signal indicates population growing with the same lifetime. The τ_2-associated spectrum simply decays as the final state is not observable.

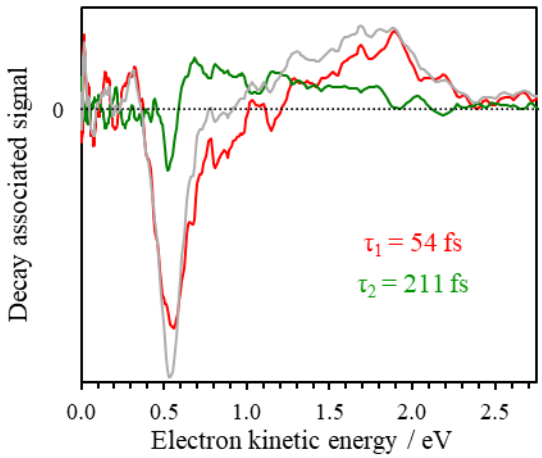

Figure 4: Decay associated spectra obtained from a global fit to the time-resolved photoelectron spectra, a selection of which was shown in Figure 3. Red and green lines represent the spectra associated with τ_1 and τ_2, respectively. The grey line is the sum of both decay associated spectra and represents the time-resolved photoelectron spectrum arising from the initially excited state.

Inspection of the τ_1-associated spectrum shows that the negative peak at eKE = 0.55 eV and a positive peak with a maximum around eKE ~ 1.9 eV. However, there is also negative signal between 0.6 < eKE < 1.2 eV. This overlaps with the τ_2-associated spectrum, showing that some signal in the 1.2 < eKE < 2.3 eV range leads to the τ_2-associated spectrum (the other fraction leads to the recovery of the bleach at 0.55 eV). For a three-state model, the time-resolved photoelectron spectrum associated with the initial excited state can be obtained by the sum of the τ_1- and τ_2-associated spectra.[56] This spectrum is also included in Figure 4.

Discussion

Two-photon resonance-enhanced photoelectron spectroscopy has previously shown the electron affinity of $[ATP–H_2]^-$ to be ADE ~ 4.1 eV.[13] Hence, excitation at $h\nu_{pu}$ = 4.66 eV is above the adiabatic energy of $[ATP–H_2]^{2-}$. This is consistent with the pump-probe spectrum in Figures 1 and 2 that shows the photoelectron extends to eKE ~ 2.1 eV. However, even though it is above the adiabatic energy, the excitation energy does not overcome the RCB. Hence, electron emission following one-photon excitation at $h\nu_{pu}$ = 4.66 eV requires the tunneling of an electron through this RCB. The initial excitation is resonant with the bright $^1\pi\pi^*$ states on adenine and it is this population that tunnels through the RCB.[13] At t = 0, some population of the $^1\pi\pi^*$ states on adenine that would otherwise have tunneled has now been projected higher in energy by $h\nu_{pr}$ =1.55 eV. Hence, a depletion is observed in the peak at eKE = 0.55 eV and a new feature is seen at higher eKE. As the total energy is above the RCB ($h\nu_{pu}$ + $h\nu_{pr}$ > ADE + RCB), this photoelectron feature is associated with direct detachment from the $^1\pi\pi^*$ states on adenine. The observed dynamics in the high eKE feature in Figure 3 is thus a reflection the population in the $^1\pi\pi^*$ states and its temporal evolution. Note that the monoanion, $[ATP–H_2]^-$, has a large electron affinity and cannot be probed by $h\nu_{pr}$. The overall dynamics are shown schematically in Figure 5.

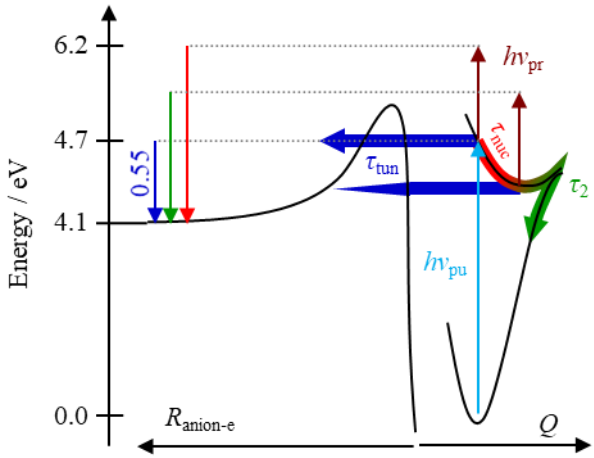

Figure 5: Schematic representation of the dynamics of $[ATP–H_2]^{2–}$ following excitation at 4.66 eV and probing at $h\nu_{pr}$ =1.55 eV. The lifetimes relate to the decays obtained from the global fit, with $\tau_1^{-1} = \tau_{tun}^{-1} + \tau_{nuc}^{-1}$.

The kinetics of the feature at eKE = 0.55 eV are mirrored by those of the feature at high eKE. This is most clearly demonstrated in Figure 4, where the decay associated spectrum of the initial process has both positive and negative components that should be interpreted as the high eKE peak that decays with τ_1 < 100 fs also leads to recovery of the peak at 0.55 eV with the same time constant. This comes about because, with increasing delay of $h\nu_{pr}$, more population has tunneled from the $^1\pi\pi^*$ states to form $[ATP–H_2]^-$. Hence, the recovery dynamics of the peak at eKE = 0.55 eV is a measure of tunneling. However, it is clear from Figure 3 that not all of the initially excited $^1\pi\pi^*$ state population decays by autodetachment, otherwise the total integrated positive and negative transient signals should cancel.[57, 58] This population can be identified in the τ_1-decay associated spectrum in Figure 4 by the negative signal between 0.8 < eKE < 1.3 eV, which shows that some population from the initially excited $^1\pi\pi^*$ states produces the photoelectron signal in this range. This range coincides with the τ_2-associated spectrum and thus shows that population flows from the initial $^1\pi\pi^*$ states (with τ_1 < 100 fs) to an intermediate that has a photoelectron spectrum given by the τ_2-associated spectrum (shown schematically in Figure 5). The fact that not all population decays by tunneling through the RCB is consistent with the conclusions of Cercola *et al.*[34], who clearly showed that photofragments

were generated following excitation at 4.66 eV. Photofragmentation is most likely a ground state process and, hence, we can associate the τ_2 decay dynamics with internal conversion from the intermediate to the ground state. The intermediate does not decay by tunneling through the RCB as this would have resulted in a negative signal associated with such dynamics. A small negative contribution can be seen in the τ_2-associated spectrum in Figure 4, suggesting that perhaps a small fraction of the population can still tunnel. We suspect that this appears because of inaccuracies in the global fitting procedure because Figure 3 does not show a similar negative signal. Nevertheless, if this signal was real then it only amounts to 10% of the observable intermediate population. Note also that the spectral shape of this transient suggests that we are probably not probing all the population of the intermediate and that some signal is likely cut-off by an RCB at lower eKE, as can be seen at eKE = 0.55 eV in the τ_2-associated spectrum. In order to observe a larger portion of the intermediate, we have attempted to repeat the experiments with $h\nu_{pr}$ =3.10 eV, but these experiments were unsuccessful. Hence, we conclude that the majority (*i.e.* >90 %) of the intermediate state population decays by internal conversion to the ground electronic state.

Note that the observed τ_1 dynamics arise from competing dynamics: decay by tunneling (τ_{tun}) and decay by nuclear motion on the $^1\pi\pi^*$ states (τ_{nuc}), as shown in Figure 5. The τ_1 lifetime is thence defined by $\tau_1^{-1} = \tau_{tun}^{-1} + \tau_{nuc}^{-1}$. Unfortunately, we cannot independently determine τ_{tun} and τ_{nuc}.

The τ_2-associated spectrum is that of the intermediate produced (Figure 5). To assign the nature of the intermediate, we consider two likely processes. First, the initially populated vibrational wavepacket moves on the $^1\pi\pi^*$ surface away from the Franck-Condon region to this transient state. Second, initial motion on the $^1\pi\pi^*$ surface can lead to internal conversion to a nearby $^1n\pi^*$ state through a conical intersection. The role and the relative position of the optically dark $^1n\pi^*$ state has been extensively debated for nucleobases and nucleotides.[12, 59, 60] We have previously calculated that the $^1n\pi^*$ state lies about 0.3 eV lower in energy than the $^1\pi\pi^*$ state in $[ATP–H_2]^{2–}$. For the case of deprotonated deoxyadenosine monophosphate ($dAMP^–$), the two states are very close in energy.[12] However, it should be noted that the relative energies depend sensitively on the level of theory used.

The $^1n\pi^*$ state could also decrease in energy in proximity of a conical intersection, as happens in the case of isolated Ade and 9-methyl-adenine (9-Me-Ade).[12, 61] Finally, the relative energies between the $^1\pi\pi^*$ and $^1n\pi^*$ states differs in differing environments: in aqueous solution, the $^1n\pi^*$ state increase in energy for Ade, 9-Me-Ade and $dAMP^-$.[62-64]

The decay mechanism of $[ATP–H_2]^{2-}$ bears close similarities with that of $dAMP^-$. The time-resolved photoelectron spectroscopy of $dAMP^-$, excited at 4.66 eV and probed at 3.10 eV, could similarly be fitted with a 3-state model with lifetimes of $\tau_1 \sim 30$ fs and $\tau_2 = 290$ fs.[12] These values are similar to those observed here, where τ_1 is less than the cross-correlation and $\tau_2 = 210$ fs. However, the most striking similarities are between the decay-associated spectra. The τ_1-associated spectrum has a similar overall spectral shape peaking at high eKE as seen in Figure 4, while obviously no tunneling takes place in $dAMP^-$ and therefore no negative peak at 0.55 eV was observed, although some negative signal was seen indicating that the initial population decays into an intermediate. The τ_2-associated spectrum of the intermediate of $dAMP^-$ is also remarkably similar in $[ATP–H_2]^{2-}$. This offers some evidence that the same intermediate is formed in both cases and that the decay from this intermediate is similar. For $dAMP^-$, evidence could be given to support that the intermediate seen corresponds to nuclear motion on the $^1\pi\pi^*$ state, without any involvement of the optically dark $^1n\pi^*$ state.[12] Given the overall similarity of the observed dynamics between $dAMP^-$ and $[ATP–H_2]^{2-}$, we suggest that the intermediate in Figure 3 and 4 also corresponds to a different geometry of the $^1\pi\pi^*$ state. Note that in the study on $dAMP^-$, similarities between it and 9Me-Ade were drawn so that we conclude that the dynamics are in fact very similar to those of just the nucleobase.

It is perhaps surprising that there are such clear similarities in the dynamics between $dAMP^-$ and $[ATP–H_2]^{2-}$ (and 9Me-Ade). The negative charge has a clear effect on the energies of the π molecular orbitals of Ade relative to the ionization energies, which decrease from 8.26 eV for Ade to 5.65 eV for $dAMP^-$ to 4.1 eV for $[ATP–H_2]^{2-}$. Nevertheless, the excited $^1\pi\pi^*$ states appear at approximately the same excitation energy, and their dynamics – which one might envisage being very sensitive to any external factors such as nearby negative charges – are very similar. Hence, while the

energies of the π molecular orbitals have changed substantially relative to the ionization energy, the relative energies between the π and π* orbitals on the Ade nucleobase appear to not have changed significantly.

Conclusions

The excited state dynamics following excitation at 4.66 eV of the isolated doubly-deprotonated dianion of ATP, $[ATP–H_2]^{2–}$, has been probed using time-resolved photoelectron spectroscopy. The initially excited $^1\pi\pi^*$ state population undergoes decay with a fraction of the population decaying by electron tunneling through the repulsive Coulomb barrier (RCB), while another fraction decays by nuclear motion on the $^1\pi\pi^*$ state, which leads to a discernable intermediate, that subsequently decays on a ~200 fs timescale by internal conversion to the ground electronic state. A global analysis reveals that the dynamics of $[ATP–H_2]^{2–}$ are similar to the dynamics observed in $dAMP^–$, where the intermediate was assigned to population on the $^1\pi\pi^*$ state surface that has moved away from the Franck-Condon region. This population can no longer tunnel through the RCB of $[ATP–H_2]^{2–}$ and decays to its ground electronic state. This excess energy then leads to fragmentation as has been observed in the photo-fragmentation action spectra reported by Cercola *et al*..[34] In a drive to understand ever larger and more complex systems, such as oligonucleotides and DNA fragments, these data offer an important glimpse into the role of electron tunneling in these systems.

Conflicts of interest

The authors declare no conflicts of interest.

Acknowledgements

Jan Verlet is grateful to Dan Neumark for the fun and productive times in the Berkeley bunkers and for his continued support over the years. This work was supported by funding from the European

Union's Horizon 2020 research and innovation program under the Marie Skłodowska-Curie grant agreement No.765266 (LightDyNAmics).

References

1. Alberts, B., *Molecular biology of the cell*. 5th ed.; Garland Science: New York, 2008.

2. Steenken, S., Purine bases, nucleosides, and nucleotides: aqueous solution redox chemistry and transformation reactions of their radical cations and e- and OH adducts. *Chem. Rev.* **1989,** *89* (3), 503-520.

3. Burrows, C. J.; Muller, J. G., Oxidative nucleobase modifications leading to strand scission. *Chem. Rev.* **1998,** *98* (3), 1109-1151.

4. Middleton, C. T.; Harpe, K. d. L.; Su, C.; Law, Y. K.; Crespo-Hernández, C. E.; Kohler, B., DNA Excited-State Dynamics: From Single Bases to the Double Helix. *Annu. Rev. Phys. Chem.* **2009,** *60* (1), 217-239.

5. Crespo-Hernández, C. E.; Cohen, B.; Hare, P. M.; Kohler, B., Ultrafast Excited-State Dynamics in Nucleic Acids. *Chem. Rev.* **2004,** *104* (4), 1977-2020.

6. de Vries, M. S.; Hobza, P., Gas-phase spectroscopy of biomolecular building blocks. *Annu. Rev. Phys. Chem.* **2007,** *58*, 585-612.

7. Stavros, V. G.; Verlet, J. R. R., Gas-Phase Femtosecond Particle Spectroscopy: A Bottom-Up Approach to Nucleotide Dynamics. *Annu. Rev. Phys. Chem.* **2016,** *67* (1), 211-232.

8. Satzger, H.; Townsend, D.; Zgierski, M. Z.; Patchkovskii, S.; Ullrich, S.; Stolow, A., Primary processes underlying the photostability of isolated DNA bases: Adenine. *Proc. Natl. Acad. Sci. U.S.A.* **2006,** *103* (27), 10196-10201.

9. Bisgaard, C. Z.; Satzger, H.; Ullrich, S.; Stolow, A., Excited-State Dynamics of Isolated DNA Bases: A Case Study of Adenine. *ChemPhysChem* **2009,** *10* (1), 101-110.

10. Wells, K. L.; Hadden, D. J.; Nix, M. G. D.; Stavros, V. G., Competing πσ* States in the Photodissociation of Adenine. *J. Phys. Chem. Lett.* **2010,** *1* (6), 993-996.

11. Mai, S.; Richter, M.; Marquetand, P.; González, L., Excitation of Nucleobases from a Computational Perspective II: Dynamics. In *Photoinduced Phenomena in Nucleic Acids I: Nucleobases in the Gas Phase and in Solvents*, Barbatti, M.; Borin, A. C.; Ullrich, S., Eds. Springer International Publishing: Cham, 2015; pp 99-153.

12. Chatterley, A. S.; West, C. W.; Roberts, G. M.; Stavros, V. G.; Verlet, J. R. R., Mapping the Ultrafast Dynamics of Adenine onto Its Nucleotide and Oligonucleotides by Time-Resolved Photoelectron Imaging. *J. Phys. Chem. Lett.* **2014,** *5* (5), 843-848.

13. Castellani, M. E.; Avagliano, D.; González, L.; Verlet, J. R. R., Site-Specific Photo-oxidation of the Isolated Adenosine-5′-triphosphate Dianion Determined by Photoelectron Imaging. *J. Phys. Chem. Lett.* **2020,** *11* (19), 8195-8201.

14. Chatterley, A. S.; Johns, A. S.; Stavros, V. G.; Verlet, J. R. R., Base-Specific Ionization of Deprotonated Nucleotides by Resonance Enhanced Two-Photon Detachment. *J. Phys. Chem. A* **2013,** *117* (25), 5299-5305.

15. Yang, X.; Wang, X.-B.; Vorpagel, E. R.; Wang, L.-S., Direct experimental observation of the low ionization potentials of guanine in free oligonucleotides by using photoelectron spectroscopy. *Proc. Natl. Acad. Sci. U.S.A.* **2004,** *101* (51), 17588-17592.

16. Wang, X.-B.; Ding, C.-F.; Wang, L.-S., Photodetachment Spectroscopy of a Doubly Charged Anion: Direct Observation of the Repulsive Coulomb Barrier. *Phys. Rev. Lett.* **1998,** *81*, 3351-3354.

17. Simons, J., Molecular Anions. *J. Phys. Chem. A* **2008,** *112* (29), 6401-6511.

18. Dreuw, A.; Cederbaum, L. S., Multiply Charged Anions in the Gas Phase. *Chem. Rev.* **2002,** *102* (1), 181-200.

19. Verlet, J. R. R.; Horke, D. A.; Chatterley, A. S., Excited states of multiply-charged anions probed by photoelectron imaging: riding the repulsive Coulomb barrier. *Phys. Chem. Chem. Phys.* **2014,** *16* (29), 15043-15052.

20. Scheller, M. K.; Compton, R. N.; Cederbaum, L. S., Gas-Phase Multiply Charged Anions. *Science* **1995,** *270* (5239), 1160-1166.

21. Wang, L.-S.; Wang, X.-B., Probing Free Multiply Charged Anions Using Photodetachment Photoelectron Spectroscopy. *J. Phys. Chem. A* **2000,** *104* (10), 1978-1990.

22. Wang, X.-B.; Wang, L.-S., Observation of negative electron-binding energy in a molecule. *Nature* **1999,** *400* (6741), 245-248.

23. Wang, X.-B.; Woo, H.-K.; Huang, X.; Kappes, M. M.; Wang, L.-S., Direct Experimental Probe of the On-Site Coulomb Repulsion in the Doubly Charged Fullerene Anion $\mathrm{C}_{70}{}^{2\ensuremath{-}}$. *Phys. Rev. Lett.* **2006,** *96* (14), 143002.

24. Dau, P. D.; Liu, H.-T.; Yang, J.-P.; Winghart, M.-O.; Wolf, T. J. A.; Unterreiner, A.-N.; Weis, P.; Miao, Y.-R.; Ning, C.-G.; Kappes, M. M.; Wang, L.-S., Resonant tunneling through the repulsive Coulomb barrier of a quadruply charged molecular anion. *Phys. Rev. A* **2012,** *85* (6), 064503.

25. Horke, D. A.; Chatterley, A. S.; Verlet, J. R., Effect of internal energy on the repulsive Coulomb barrier of polyanions. *Phys. Rev. Lett.* **2012,** *108* (8), 083003.

26. Horke, D. A.; Chatterley, A. S.; Verlet, J. R. R., Femtosecond Photoelectron Imaging of Aligned Polyanions: Probing Molecular Dynamics through the Electron–Anion Coulomb Repulsion. *J. Phys. Chem. Lett.* **2012,** *3* (7), 834-838.

27. Horke, D. A.; Chatterley, A. S.; Verlet, J. R. R., Influence of the repulsive Coulomb barrier on photoelectron spectra and angular distributions in a resonantly excited dianion. *J. Chem. Phys.* **2013,** *139* (8), 084302.

28. Gabelica, V.; Tabarin, T.; Antoine, R.; Rosu, F.; Compagnon, I.; Broyer, M.; De Pauw, E.; Dugourd, P., Electron photodetachment dissociation of DNA polyanions in a quadrupole ion trap mass spectrometer. *Anal. Chem.* **2006,** *78* (18), 6564-72.

29. Gabelica, V.; Rosu, F.; Tabarin, T.; Kinet, C.; Antoine, R.; Broyer, M.; De Pauw, E.; Dugourd, P., Base-dependent electron photodetachment from negatively charged DNA strands upon 260-nm laser irradiation. *J. Am. Chem. Soc.* **2007,** *129* (15), 4706-13.

30. Rosu, F.; Gabelica, V.; De Pauw, E.; Antoine, R.; Broyer, M.; Dugourd, P., UV spectroscopy of DNA duplex and quadruplex structures in the gas phase. *J. Phys. Chem. A* **2012,** *116* (22), 5383-91.

31. Schinle, F.; Crider, P. E.; Vonderach, M.; Weis, P.; Hampe, O.; Kappes, M. M., Spectroscopic and theoretical investigations of adenosine 5'-diphosphate and adenosine 5'-triphosphate dianions in the gas phase. *Phys. Chem. Chem. Phys.* **2013,** *15* (18), 6640-50.

32. Burke, R. M.; Dessent, C. E. H., Effect of Cation Complexation on the Structure of a Conformationally Flexible Multiply Charged Anion: Stabilization of Excess Charge in the Na+·Adenosine 5′-Triphosphate Dianion Ion-Pair Complex. *J. Phys. Chem. A* **2009,** *113* (12), 2683-2692.

33. Burke, R. M.; Pearce, J. K.; Boxford, W. E.; Bruckmann, A.; Dessent, C. E. H., Stabilization of Excess Charge in Isolated Adenosine 5‘-Triphosphate and Adenosine 5‘-Diphosphate Multiply and Singly Charged Anions. *J. Phys. Chem. A* **2005,** *109* (43), 9775-9785.

34. Cercola, R.; Matthews, E.; Dessent, C. E. H., Photoexcitation of Adenosine 5′-Triphosphate Anions in Vacuo: Probing the Influence of Charge State on the UV Photophysics of Adenine. *J. Phys. Chem. B* **2017,** *121* (22), 5553-5561.

35. Vonderach, M.; Ehrler, O. T.; Matheis, K.; Weis, P.; Kappes, M. M., Isomer-Selected Photoelectron Spectroscopy of Isolated DNA Oligonucleotides: Phosphate and Nucleobase Deprotonation at High Negative Charge States. *J. Am. Chem. Soc.* **2012,** *134* (18), 7830-7841.

36. Weber, J. M.; Ioffe, I. N.; Berndt, K. M.; Löffler, D.; Friedrich, J.; Ehrler, O. T.; Danell, A. S.; Parks, J. H.; Kappes, M. M., Photoelectron Spectroscopy of Isolated Multiply Negatively Charged Oligonucleotides. *J. Am. Chem. Soc.* **2004,** *126* (27), 8585-8589.

37. Daly, S.; Rosu, F.; Gabelica, V., Mass-resolved electronic circular dichroism ion spectroscopy. *Science* **2020,** *368* (6498), 1465-1468.

38. Ullrich, S.; Schultz, T.; Zgierski, M. Z.; Stolow, A., Direct Observation of Electronic Relaxation Dynamics in Adenine via Time-Resolved Photoelectron Spectroscopy. *J. Am. Chem. Soc.* **2004,** *126* (8), 2262-2263.

39. Chatterley, A. S.; West, C. W.; Stavros, V. G.; Verlet, J. R. R., Time-resolved photoelectron imaging of the isolated deprotonated nucleotides. *Chem. Sci.* **2014,** *5* (10), 3963-3975.

40. Canuel, C.; Mons, M.; Piuzzi, F.; Tardivel, B.; Dimicoli, I.; Elhanine, M., Excited states dynamics of DNA and RNA bases: characterization of a stepwise deactivation pathway in the gas phase. *J. Chem. Phys.* **2005,** *122* (7), 074316.

41. Kang, H.; Lee, K. T.; Jung, B.; Ko, Y. J.; Kim, S. K., Intrinsic lifetimes of the excited state of DNA and RNA bases. *J. Am. Chem. Soc.* **2002,** *124* (44), 12958-9.

42. Nix, M. G. D.; Devine, A. L.; Cronin, B.; Ashfold, M. N. R., Ultraviolet photolysis of adenine: Dissociation via the π1σ* state. *J. Chem. Phys.* **2007,** *126* (12), 124312.

43. Kleinermanns, K.; Nachtigallová, D.; de Vries, M. S., Excited state dynamics of DNA bases. *Int. Rev. Phys. Chem.* **2013,** *32* (2), 308-342.

44. Serrano-Andrés, L.; Merchán, M.; Borin, A. C., Adenine and 2-aminopurine: paradigms of modern theoretical photochemistry. *Proc. Natl. Acad. Sci. U.S.A.* **2006,** *103* (23), 8691-8696.

45. Barbatti, M.; Aquino, A. J. A.; Szymczak, J. J.; Nachtigallová, D.; Hobza, P.; Lischka, H., Relaxation mechanisms of UV-photoexcited DNA and RNA nucleobases. *Proc. Natl. Acad. Sci. U.S.A.* **2010,** *107* (50), 21453-21458.

46. Barbatti, M.; Lischka, H., Nonadiabatic Deactivation of 9H-Adenine: A Comprehensive Picture Based on Mixed Quantum−Classical Dynamics. *J. Am. Chem. Soc.* **2008,** *130* (21), 6831-6839.

47. Barbatti, M.; Lan, Z.; Crespo-Otero, R.; Szymczak, J. J.; Lischka, H.; Thiel, W., Critical appraisal of excited state nonadiabatic dynamics simulations of 9H-adenine. *J. Chem. Phys.* **2012,** *137* (22), 22a503.

48. Serrano-Andrés, L.; Merchán, M., Are the five natural DNA/RNA base monomers a good choice from natural selection?: A photochemical perspective. *J. Photochem. Photobiol. C* **2009,** *10* (1), 21-32.

49. Improta, R.; Santoro, F.; Blancafort, L., Quantum Mechanical Studies on the Photophysics and the Photochemistry of Nucleic Acids and Nucleobases. *Chem. Rev.* **2016,** *116* (6), 3540-3593.

50. Lecointre, J.; Roberts, G. M.; Horke, D. A.; Verlet, J. R. R., Ultrafast Relaxation Dynamics Observed Through Time-Resolved Photoelectron Angular Distributions. *J. Phys. Chem. A* **2010,** *114* (42), 11216-11224.

51. Stanley, L. H.; Anstöter, C. S.; Verlet, J. R. R., Resonances of the anthracenyl anion probed by frequency-resolved photoelectron imaging of collision-induced dissociated anthracene carboxylic acid. *Chem. Sci.* **2017,** *8* (4), 3054-3061.

52. Wiley, W. C.; McLaren, I. H., Time-of-Flight Mass Spectrometer with Improved Resolution. *Rev. Sci. Instrum.* **1955,** *26* (12), 1150-1157.

53. Horke, D. A.; Roberts, G. M.; Lecointre, J.; Verlet, J. R. R., Velocity-map imaging at low extraction fields. *Rev. Sci. Instrum.* **2012,** *83* (6), 063101.

54. Roberts, G. M.; Nixon, J. L.; Lecointre, J.; Wrede, E.; Verlet, J. R. R., Toward real-time charged-particle image reconstruction using polar onion-peeling. *Rev. Sci. Instrum.* **2009,** *80* (5), 053104.

55. Fingerman, S., CRC handbook of chemistry and physics; a ready-reference book of chemical and physical data, 87th ed. *Sci-Tech News* **2007,** *61* (1), 38-38.

56. Mooney, C. R. S.; Horke, D. A.; Chatterley, A. S.; Simperler, A.; Fielding, H. H.; Verlet, J. R. R., Taking the green fluorescence out of the protein: dynamics of the isolated GFP chromophore anion. *Chem. Sci.* **2013,** *4* (3), 921-927.

57. Horke, D. A.; Li, Q.; Blancafort, L.; Verlet, J. R. R., Ultrafast above-threshold dynamics of the radical anion of a prototypical quinone electron-acceptor. *Nature Chem.* **2013,** *5* (8), 711-717.

58. Anstöter, C. S.; Bull, J. N.; Verlet, J. R. R., Ultrafast dynamics of temporary anions probed through the prism of photodetachment. *Int. Rev. Phys. Chem.* **2016,** *35* (4), 509-538.

59. Gustavsson, T.; Sharonov, A.; Onidas, D.; Markovitsi, D., Adenine, deoxyadenosine and deoxyadenosine 5′-monophosphate studied by femtosecond fluorescence upconversion spectroscopy. *Chem. Phys. Lett.* **2002,** *356* (1), 49-54.

60. Markovitsi, D., UV-induced DNA Damage: The Role of Electronic Excited States. *Photochem. Photobiol.* **2016,** *92* (1), 45-51.

61. Picconi, D.; Avila Ferrer, F. J.; Improta, R.; Lami, A.; Santoro, F., Quantum-classical effective-modes dynamics of the ππ* → nπ* decay in 9H-adenine. A quadratic vibronic coupling model. *Faraday Discuss.* **2013,** *163* (0), 223-242.

62. Gustavsson, T.; Sarkar, N.; Vayá, I.; Jiménez, M. C.; Markovitsi, D.; Improta, R., A joint experimental/theoretical study of the ultrafast excited state deactivation of deoxyadenosine and 9-methyladenine in water and acetonitrile. *Photochem. Photobiol. Sci.* **2013,** *12* (8), 1375-1386.

63. Improta, R.; Barone, V., The excited states of adenine and thymine nucleoside and nucleotide in aqueous solution: a comparative study by time-dependent DFT calculations. *Theoretical Chemistry Accounts* **2008,** *120* (4), 491-497.

64. Santoro, F.; Improta, R.; Fahleson, T.; Kauczor, J.; Norman, P.; Coriani, S., Relative Stability of the La and Lb Excited States in Adenine and Guanine: Direct Evidence from TD-DFT Calculations of MCD Spectra. *J. Phys. Chem. Lett.* **2014,** *5* (11), 1806-1811.

TOC graphic